Available online at www.sciencedirect.com
ScienceDirect
Continental Shelf Research 27 (2007) 1379–1398
CONTINENTAL SHELF RESEARCH
www.elsevier.com/locate/csr

Water masses in the Monterey Bay during the summer of 2000

Alex Warn-Varnas[a,*], Avijit Gangopadhyay[b], J.A. Hawkins[c]

[a]*Naval Research Laboratory, Stennis Space Center, MS 39529, USA*
[b]*School for Marine Science and Technology, Department of Physics, University of Massachusetts Dartmouth, 285 Old Westport Road, North Dartmouth, MA 02747, USA*
[c]*Planning Systems Inc., Slidell, LA 70458, USA*

Received 8 June 2005; received in revised form 9 November 2006; accepted 3 January 2007
Available online 19 January 2007

Abstract

Water masses in Monterey Bay are determined from the CTD casts of the Monterey Ocean Observing System (MOOS) Upper-water-column Science Experiment (MUSE) August 2000 dataset. It is shown through cluster analysis that the MUSE 2000 CTD dataset contains 5 water masses. These five water masses are: bay surface water (BSW), bay warm water (BWW), bay intermediate water (BIW), sub arctic upper water (SUW) and North Pacific deep water (NPDW). The BWW is a new water mass that exists in one area and is attributed to the effects of solar heating. The volumes occupied by each of the water masses are obtained. The BIW water is the most dominant water mass and occupies 68.8% of the volume. The statistical means and standard deviations for each water parameter, including spiciness and oxygen concentration, are calculated during separate upwelling and relaxed periods.

The water mass content and structure are analyzed and studied during upwelling and a relaxed period. During upwelling, along a CTD track off Pt. Ano Nuevo, the water mass T, S distribution tended to be organized along three branches. Off Pt. Ano Nuevo the innovative coastal observation network (ICON) model showed the formation of a cyclonic eddy during the analyzed upwelling period. In time the eddy moved southwest and became absorbed into the southerly flow during the initial phases of the following wind-relaxed period.

1. Introduction

The physical oceanography off the coast of California includes an offshore region and a dynamic coastal region. The offshore region is primarily dominated by the large-scale California current (CC), the California under current (CUC) and parts of the subtropical and subpolar gyre circulations of the eastern Pacific (Hickey, 1979). There are very energetic shallow water features in the coastal transition zone (CTZ) around the coastal area of Monterey Bay and the California current system (Breaker and Broenkow, 1994). There are filaments, coastal eddies, anomalous pools, jets along the upwelling fronts (Rosenfeld et al., 1994) and mushroom-like vortices (Mied et al., 1991), all of which contribute to the scales and variability of the synoptic circulation in the region.

The topography of the Monterey Bay region is complex. Near the coast there is a shallow layer of 150 m or less. Away from the coast the depths increase to 2 km or more. In the bay area, the head

*Corresponding author. Tel.: +1 228 688 4870; fax: +1 228 688 4759.
E-mail address: varnas@nrlssc.navy.mil (A. Warn-Varnas).

0278-4343/$ - see front matter © 2007 Elsevier Ltd. All rights reserved.
doi:10.1016/j.csr.2007.01.004

of the Monterey Submarine Canyon is located. The effects of the canyon on the circulation have been studied. Rosenfeld et al. (1994) found that the canyon had no influence on SSTs in the bay. Other authors suggest that upwelling through the canyons is important at other depths, (e.g., Shea and Broenkow, 1982; Hickey, 1997).

Next to the offshore region is the large-scale domain that encompasses the Pacific Ocean water masses and circulation. There the eastern North Pacific central water (ENPCW) is found. To the west, adjacent to the ENPCW is the domain of the western North Pacific central water (WNPCW). These water masses span potential density surfaces, σ_θ, 25.5–26.5. On the northern side, the WNPCW and ENPCW extend to the subtropical convergence zone. On the eastern side they extend to a transition zone along the California coast. The sub arctic upper water (SUW) is carried into the area by the eastern boundary current along the subtropical gyre (Tomczak and Godfrey, 1994).

It is challenging to understand the various aspects of the synoptic variability of the prevalent circulation features in the Monterey Bay and its adjacent areas, including the California current system (CCS). This is so even when one focuses only on the summer (July–August) season. Some of the complexities arise from the dynamic behavior of the CCS as well as its interactions with the highly variable shelf circulation and the wind-driven upwelling processes. The coastal transition zone that separates the shelf circulation from the offshore flows was studied in the late 1980s and early 1990s, giving rise to even more questions (Brink et al., 1991; Strub et al., 1991).

Generally, the summer circulation in the Monterey Bay is distinguished by two distinct phases of wind-driven upwelling for about 1–3 weeks followed by a wind-relaxed period of anywhere from 3 to 6 d. During sustained upwelling, there are distinct upwelling centers near Pt Ano Neuvo and Pt Sur. Sometimes, the upwelling signature off of Pt Ano Neuvo has distinct bifurcating filaments, one alongshore and the other normal to the shore (Rosenfeld et al., 1994), mostly due to the two distinct wind components, which are both capable of creating sizable Ekman drifts. A cyclonic circulation is observed inshore of the front in the bay, while the offshore circulation has an anticyclonic eddy-like feature. See Table 1 for a list of prevalent features and some relevant studies. The relaxed period is more of an adjustment period of the transient features generated during the upwelling cycle.

The objective of this paper is to determine the water masses and interpret their structure in terms of predicted circulation features, near and around Monterey Bay, for the period of August 2000. Two particular aspects of water mass signatures are of interest: (1) to characterize the prevalent water masses and compare their ranges during upwelling and relaxed periods, and (2) to introduce the concept of spiciness (Rudnick and Ferrari, 1999; Ferrari and Rudnick, 2000; Flament, 2002), and thus describe the various water masses in the CTZ and relate these water masses to the shallow water features.

One of our long-term goals is use zero-order dynamical processes to describe the characteristics of the 'features'. Since the spiciness bounds the T–S

Table 1
Circulation features in the Monterey Bay region during upwelling and relaxed periods

Temporal scale	Upwelling state	Relaxed state	References
	1–2 weeks	3–6 d	
Features	Bifurcating upwelling frontal system from Pt. Ano Neuvo	Offshore advection	Rosenfeld et al. (1994); Ramp et al. (1997); Rosenfeld et al. (1995)
	Anticyclonic eddy on the offshore side of the offshore upwelling filament	Anticyclonic eddy moves onshore	Tracy (1990) and others previously noted in working paper
	Cyclonic circulation in the bay	Cyclone reduces in extent (probably intensify)	Tracy (1990) and others previously noted in working paper on CCS (Gangopadhyay et al., 2006)
	Bifurcating upwelling frontal system from Pt. Sur	Transient features in the bay	Traganza et al. (1981); Tisch and Ramp (1997) and others

curves in the orthogonal direction to the density lines, predetermining spiciness values for a specific feature, along with an SST observation will contribute to determining the salinity and in turn the density inference. Second, the features such as filaments, jets, and mushroom-vortices are related to specific dynamical processes like instability, upwelling and wind driving. Processes such as these can be investigated and incorporated into water mass-based feature models. Niiler et al. (1989) used the spiciness criterion to describe the intrusion of low salinity and cold water through subduction into shoreward advecting filaments. In this paper, we begin the first step towards our long-term goal of using spiciness and water mass distribution to infer the existence of features and possible extrapolation in the vertical for usage in a real-time nowcasting and forecasting exercise. Towards this end, we analyze the spiciness structure of an eddy generated at the upwelling core and look closely at the negative spiciness of the SUW during upper-water-column science experiment (MUSE).

The paper is divided into different sections, as follows: Section 2 focuses on the dataset and water mass distribution in the bay; Section 3 addresses the water masses during upwelling and relaxed periods; Section 4 considers the dynamical interpretation of the water mass distribution; and Section 5 contains a discussion of the results and the conclusion.

2. Bay water masses and their distribution

2.1. Data

A large-scale oceanographic field experiment, named Monterey Ocean Observing System (MOOS) MUSE took place in Monterey Bay in August of 2000. The survey was extensive, involving eighteen collaborative research groups from thirteen institutions (www.mbari.org/muse). Three ships, two aircraft and small boats participated in the survey. The instrumentation consisted of nine moorings, six gliders, two AUVs, an ROV, and drifters. The CTD stations were designed to provide a bay-wide description of the temperature-salinity distribution during the period. Fig. 1 shows the location of the 66 CTD stations and Table 2 provides the timeline. The depths of the CTD stations varied. For analysis purposes only the top 200 m or less was used (less when topography was less than 200 m). The cruise period was during the later half of August (19–31/8). The first bay-wide survey (19–22/8; stations 1–16) was during an upwelling event. The second bay-wide survey (23–24/8; stations 17–26) was during a short break from upwelling. During the next two days (25–26/8; stations 27–32) a transect survey was carried out to focus on the upwelling region off of Pt. Ano Neuvo. The last transect survey (27–31/8; stations 33–66) was during the final wind-relaxation phase, when the offshore waters were sampled along a northwest–southwest section. The color-coding indicates these four different periods of survey in Fig. 1. The CTD dataset was derived from the three ships and processed by the MBARI group for public distribution. Prior to performing the cluster analysis, we checked the data for any outlier and found none.

2.2. Characteristics of water masses

Following Warn-Varnas et al. (2005) cluster analysis of hydrographic data are used for identifying water masses. The technique groups observations into temperature, salinity, and depth clusters that can be associated with individual water masses by using the existing knowledge base in the area (Kim et al., 1991).

The approach is objective and uses a distance function in order to combine cluster points consisting of temperature, salinity, and depth. The distance function is defined as the following:

$$F_D = T_n^2 + S_n^2 + d_n^2,$$

where $T_n = \Delta T_c/\sigma_T$, $S_n = \Delta S_c/\sigma_S$, and $d_n = \Delta d_c/\sigma_d$ are the temperature, salinity, and depth between clusters and σ_T, σ_S and σ_d are the corresponding standard deviations. The subscripts T, S, and d refer to temperature, salinity, and depth. The subscript c refers to cluster and n to the number of clusters.

The procedure consists of combining the closest two clusters into a new one until the total cluster number reaches a designated level. The average linkage method is applied to measure the distance between clusters. This method computes the distance function using the means of each cluster.

The cluster analysis is applied to the top 200 m of the dataset described in Section 2.1. Once the data were combined into five clusters, a number based on prior and present physical knowledge (the five water masses are described bellow), the analysis was stopped. The results in the T, S, D space are shown in Fig. 2 in terms of ellipsoids associated with each water mass. The mean of each water mass is

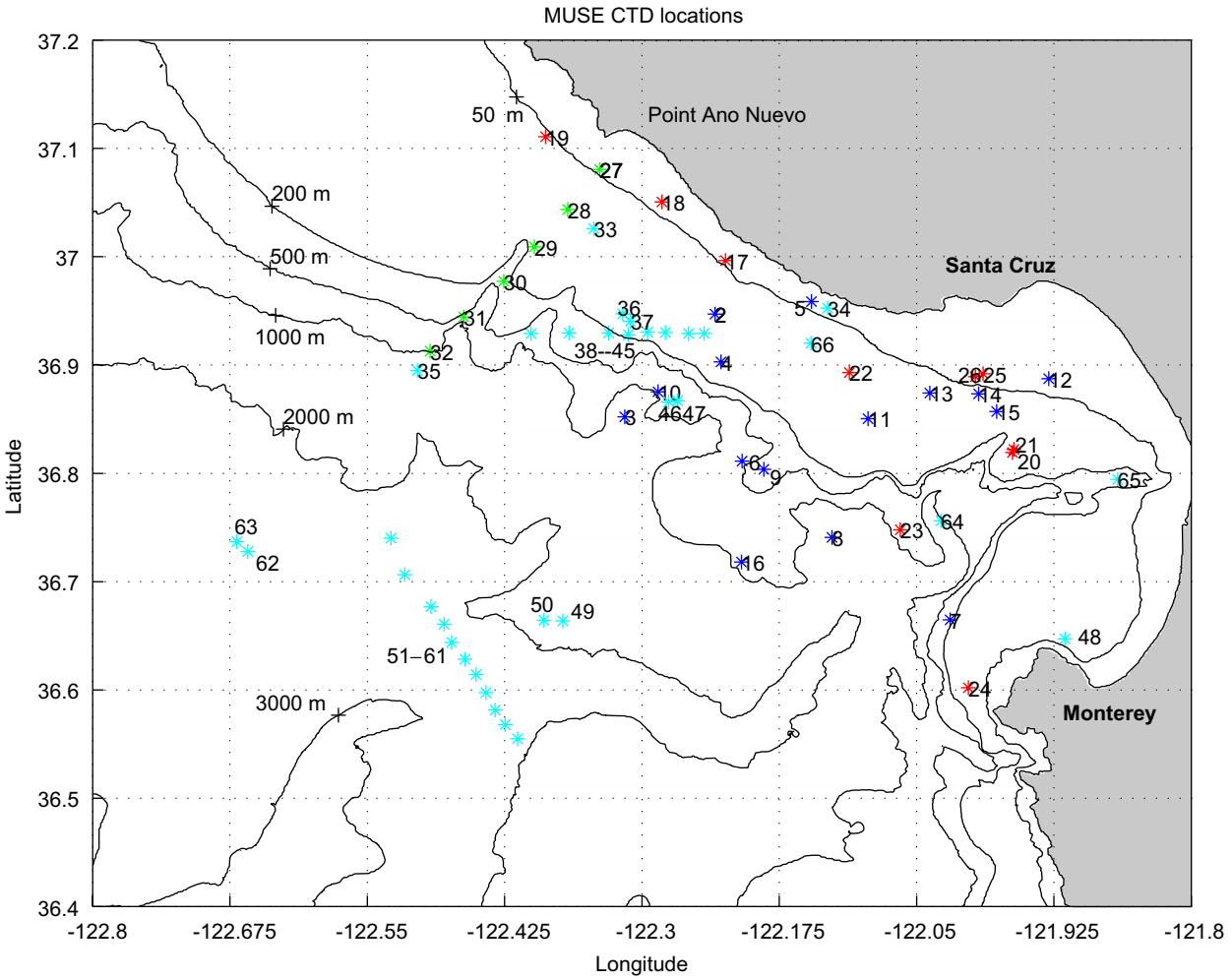

Fig. 1. Locations of CTD stations. The stations are grouped into upwelling and relaxed periods, Table 2. The color coding indicates: Blue CTD stations 2–6, U1 period in Table 2; Green CTD's 27–32, U2; red CTD's 17–26, R1; cyan CTD's 33–66, R2.

extracted from its cluster of points. The axes of the ellipsoids are the standard deviations about the mean. There are two surface water masses. We labeled one of them bay surface water (BSW), and another warmer mass, bay warm water (BWW). The deduction of BWW is based on its T, S properties. Below the surface water masses, there is the bay intermediate water (BIW), and another water mass, colder and fresher, which is labeled SUW. At the bottom is the North Pacific deep water (NPDW). Tomczak and Godfrey (1994) discuss the presence of the NPDW and SUW water masses in the region of Monterey Bay.

A projection of the water masses cluster of points on to the T, S plane is shown in Fig. 3. The color-coding indicates the water mass to which each cluster of points belong. Also shown are the 2-dimensional ellipses associated with each water mass cluster of points. They are centered on the means with standard deviations defining the axes. The BWW water occupies a unique area in the T, S space with particular spiciness values. Proceeding from the warm surface water BWW, downward (Figs. 2 and 3), the mean temperatures and the salinities of each water mass behave as expected with the exception of the SUW. This water has a lower salinity than the BIW water at a similar depth range.

Shown in the background of Fig. 3 are the potential density and spiciness contours. The concept of spiciness was originally introduced by Veronis (1972) as a quantity that is orthogonal to potential–density curves in the TS plane. Spiciness is defined in terms of the density ratio ($\alpha\Delta T/\beta\Delta S$)

where α and β are the corresponding expansion coefficients. In Veronis (1972), it was noted that the behavior of spiciness and potential density contours can provide information on vertical and horizontal mixing, and that spiciness can serve as a tracer of abyssal water masses. Flament (1986) defined and constructed spiciness as a state variable most sensitive to isopycnal thermohaline variations and least correlated with the density field. He pointed out the spiciness state variable is useful as an indicator of water masses and double-diffusive stability. Rudnick and Ferrari (1999) studied horizontal thermohaline variations and showed that temperature and salinity gradients on horizontal scales of 20 m–10 km tend to compensate in their effects on density.

Table 2
Upwelling and relaxing periods in Monterey Bay during 2000 and associated CTD observations

Date	CTD Stn	U/R
19/8	1	
20/8	2–16	U1
21/8		
22/8		
23/8	17–26	R1
24/8	(17–19)	
25/8	27–32	U2
26/8		
27/8	33–66	R2
28/8	(33–45)	
29/8		
30/8		
31/8		

The CTD #s in parenthesis above were the ones that were selected for analysis for the upwelling and relaxing period water mass comparison.
U1: uwelling period (1)
U2: upwelling period (2)
R1: relaxed period (1)
R2: relaxed period (2)

Spiciness contours are constructed following Fofonoff (1985) and Veronis (1972). They are orthogonal to the potential density contours. The magnitudes of the potential density contours range from 24.5 to 26.5. Each of the 5 water masses is bounded by a range of potential density. None of them actually lay on any particular potential density contour.

On the other hand, the spiciness contours range from +1 to −0.5. The warm surface water masses have the high spiciness values. The cold and fresh arctic type water has the lowest spiciness value. The BSW and BIW water masses are bounded by a range of spiciness values, and the other water masses tend towards a particular value of spiciness. The NPDW water mass has a spiciness value of around 0.18. The SUW water mass tends towards a value of −0.15, and the BWW water mass points cluster around 1.

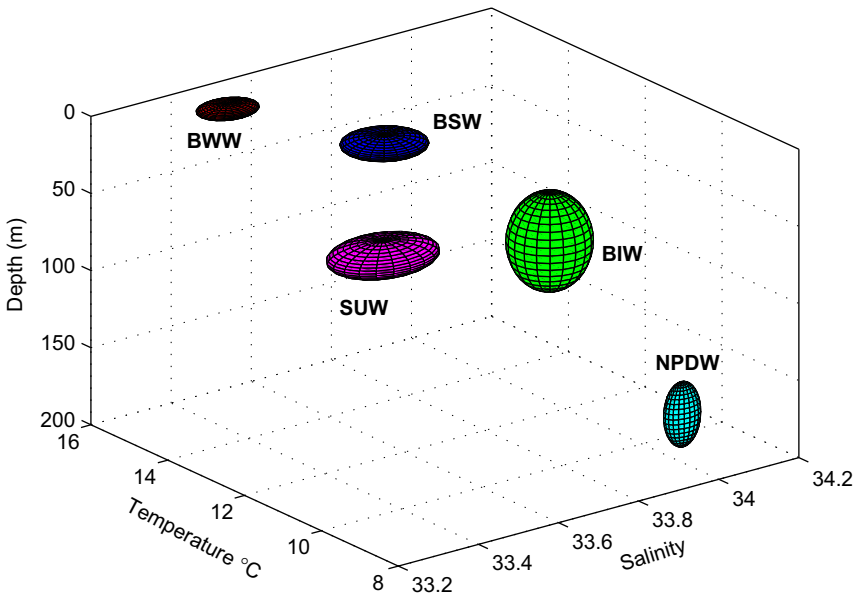

Fig. 2. Water mass ellipsoids in temperature, salinity, and depth space. The center is the mean for each water mass and the minor and major axes are the standard deviations. BWW represents the bay warm water, BSW bay surface water, BIW bay intermediate water, SUW sub arctic upper water, and NPDW North Pacific deep water.

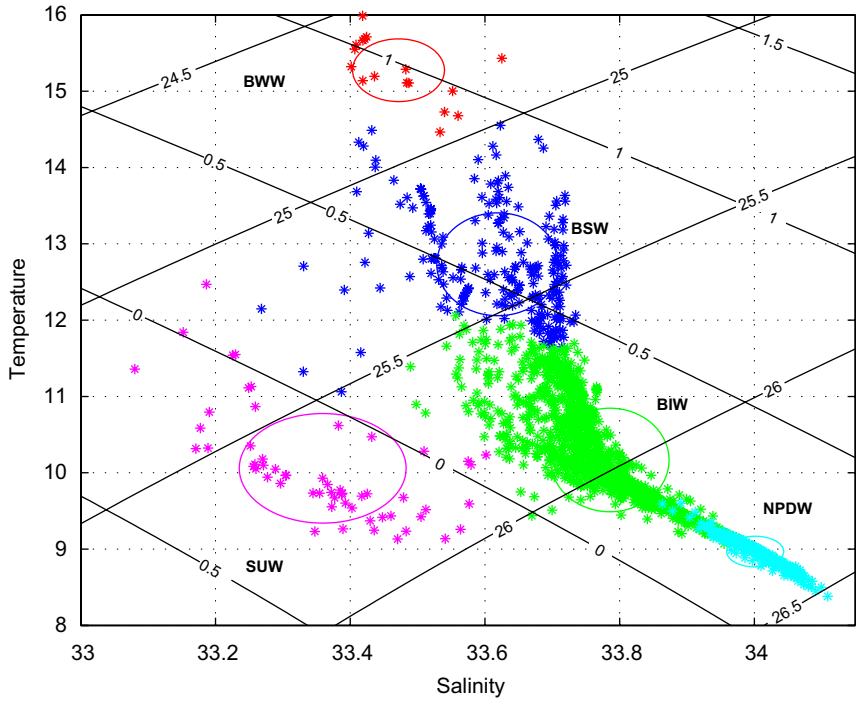

Fig. 3. *TS* diagram for water masses with ellipsoids, density and spiciness contours are shown in the background. Acronym are the same as in Fig. 2. The color coding is: red BWW, blue BSW, green BIW, pink SUW, cyan NPDW. Potential density and spiciness contours are shown in the background.

Table 3
Statistics of measured and derived water mass quantities

Water mass	No. of samples	Mean D	σ_D	Mean T	σ_T	Mean S	σ_S	Mean O_2	σ_{O^2}	Mean σ	σ_σ	Mean τ	σ_r
BWW	17	6.0	3.52	15.28	0.41	33.47	0.07	6.41	0.76	24.73	0.13	0.98	0.07
BSW	239	9.8	5.90	12.73	0.67	33.62	0.09	7.02	0.87	25.37	0.017	0.56	0.13
BIW	1390	55.17	31.7	10.17	0.68	33.79	0.09	3.73	1.06	25.97	0.18	0.21	0.07
SUW	57	33.5	10.24	10.06	0.72	33.36	0.12	5.08	0.45	25.66	0.20	−0.15	0.10
NPDW	258	168.9	20.9	8.97	0.20	34.00	0.04	2.13	0.18	25.34	0.06	0.18	0.01

The statistics of the water masses are summarized in Table 3. Each state variable is associated with the cluster of points describing the water mass in T, S, D space. The spiciness and oxygen (discussed in Section 2.5) are obtained for the particular T, S, D cluster sets describing the water masses. The means, ranges, and standard deviations of each state variable for each water mass are listed.

2.3. Distribution and volumetric analysis

The vertical extent or percent of the water column occupied by each of the water masses at the CTD casts in Monterey Bay was considered. The vertical extent or depth span occupied by a particular water mass was obtained from the cluster analysis. Then, a percentage of the water column occupied by the water mass was computed relative to the column depth as

$$\alpha_m = \frac{d_m}{D},$$

where d_m is the particular water mass depth range and D is the depth of the water column at the station. The analysis is conducted for the upper 200 m. For CTD depths less than 200 m, the CTD depth is used.

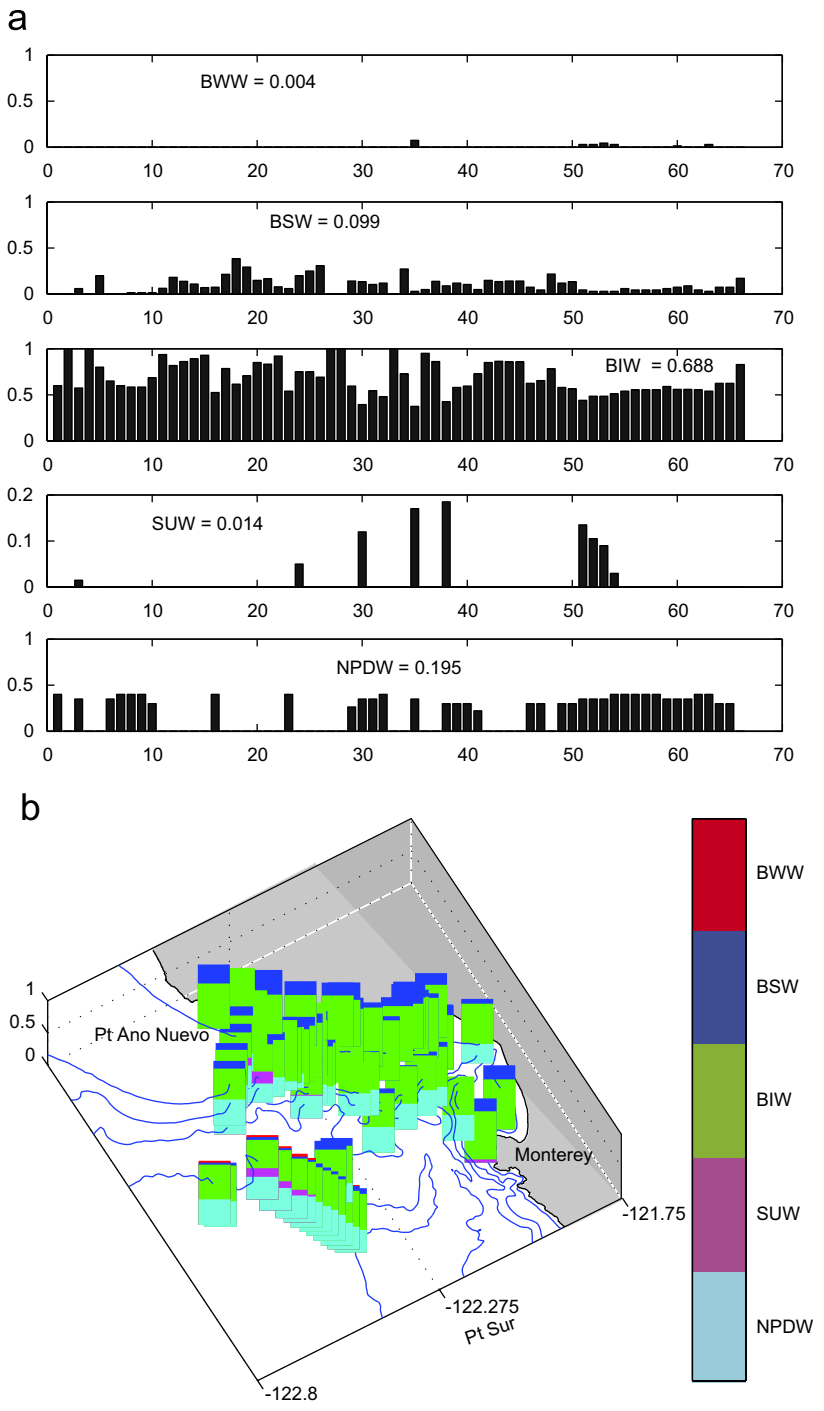

Fig. 4. (a) Bar diagrams showing fraction of water column occupied by each water mass at the respective CTD station. The fraction of volume occupied by each water mass for all CTD stations is shown on top. (b) Fraction of volume occupied by each water mass at the CTD stations as a function of latitude and longitude. Contours are the same as in Fig. 1.

The fraction of the water column occupied by each of the water masses is shown in Fig. 4(a), in terms of a bar diagram at the CTD stations taken in Monterey Bay. The BIW water mass occupies the largest percentage of the water columns with a total percentage of 68.8%. The NPDW water mass

follows with 19.5%. The BSW water mass accounts for 9.9% of the surface water. The BWW water mass occupies 0.4% of the water columns and is found only at a few CTD stations, where the warm temperatures exist for the time period of the dataset. The SUW water mass is rare and not present at all of the CTD stations. It occupies 1.4% of the water columns.

The fraction of the water column occupied by the water masses are shown in Fig. 4(b) as a geographic distribution in latitude and longitude. Analysis of Figs. 4(a) and (b) indicates that three water masses, BSW, BIW, and NPDW, were present at most of the survey stations throughout the Monterey Bay. At stations 2, 4, 27, 28, and 33, only one water mass is observed—BIW.

2.4. Origin, formation, and modification of Monterey Bay water masses

Fig. 4(b) provides a geographical insight into the water mass distribution in the Monterey Bay area during August 2000. The BIW water mass has a prevalent dominance throughout the area. Most of the time, BIW is located between the BSW and NPDW water masses. It is derived from mixing between the BSW and NPDW water masses (see Fig. 3). The controlling process is turbulent mixing in the shear zone, resulting in diapycnal and isopycnal mixing Table 4. Breaker and Broenkow (1994) outlined a three-layered circulation system in Monterey bay. The surface flow is cyclonic, at intermediate depth the flow is anticyclonic, and at deeper levels is again cyclonic. The intermediate depth flow can represent the domain of BIW mass. Above and below the BIW mass there would be shear zones induced by the reverse circulation.

Another phenomena that can contribute to the modification of BIW water is the breaking of internal bores at the Monterey Bay submarine canyon head (Breaker and Broenkow, 1994). The breaking internal bores can generate turbulence and mixing.

In the vicinity of the Monterey Bay submarine canyon, Petruncio et al. (1998) observed internal tidal effects that caused large displacements of the isopycnals. Significant internal tides can occur over the shelf. The effect of the internal tide on our analysis is primarily through vertical advection (and some horizontal advection). This will not have much effect on the water mass analysis, except possibly stretch the water mass ellipses in the vertical (Rosenfeld, pers. commun.). The main effect of the internal tides is an up and down displacement of the water masses. The measurements of Lien and Gregg (2001) show strong turbulence in a ray path along the internal tidal beam. The interaction mechanism of the beam with the surroundings enhances mixing.

The NPDW water mass is formed offshore in the North Pacific. It is advected into the bay area, by a cyclonic circulation in the deeper layers (Breaker and Broenkow, 1994). There, it undergoes mixing with the water masses in the bay area. NPDW water is also brought into the bay area by bathymetric uplifting through the Monterey Bay submarine canyon head (Breaker and Broenkow, 1994). The relatively cool, fresh SUW water is transported into the region by the equatorward California along shore current. It has a low salinity signature at its depth range (Fig. 3). In the bay area, it undergoes mixing.

The California along-shore current advects water into the bay area, where the water is subject to atmospheric forcing. The resultant mixed layer interfaces the surface layer with the BIW water mass below. Shear zones are expected to exist at the bottom of the mixed layer. The BWW warm surface water mass is located at the fringes of the bay area (Fig. 4b). The BWW warm surface water mass exists for the time period of the dataset. Its warmer

Table 4
Monterey Bay water masses

Water mass	Origin/formation	Controlling processes [formation] {modification}
BWW	Atmospheric forcing acting on surface region	{[Solar heating]}
BSW	Inflow of California current	[Advection] {atmospheric forcing} {mixed layer dynamics}
BIW	Derived from mixture of BSW and NPDW	{[Turbulent mixing in shear zone]} {isopycnal and diapycnal mixing} {breaking internal waves}
SUW	Transport of sub arctic water into bay region	[Advection] {mixing}
NPDW	Transport of NPDW into bay region	[Mesoscale dynamics] [bathymetric uplifting] {mixing}

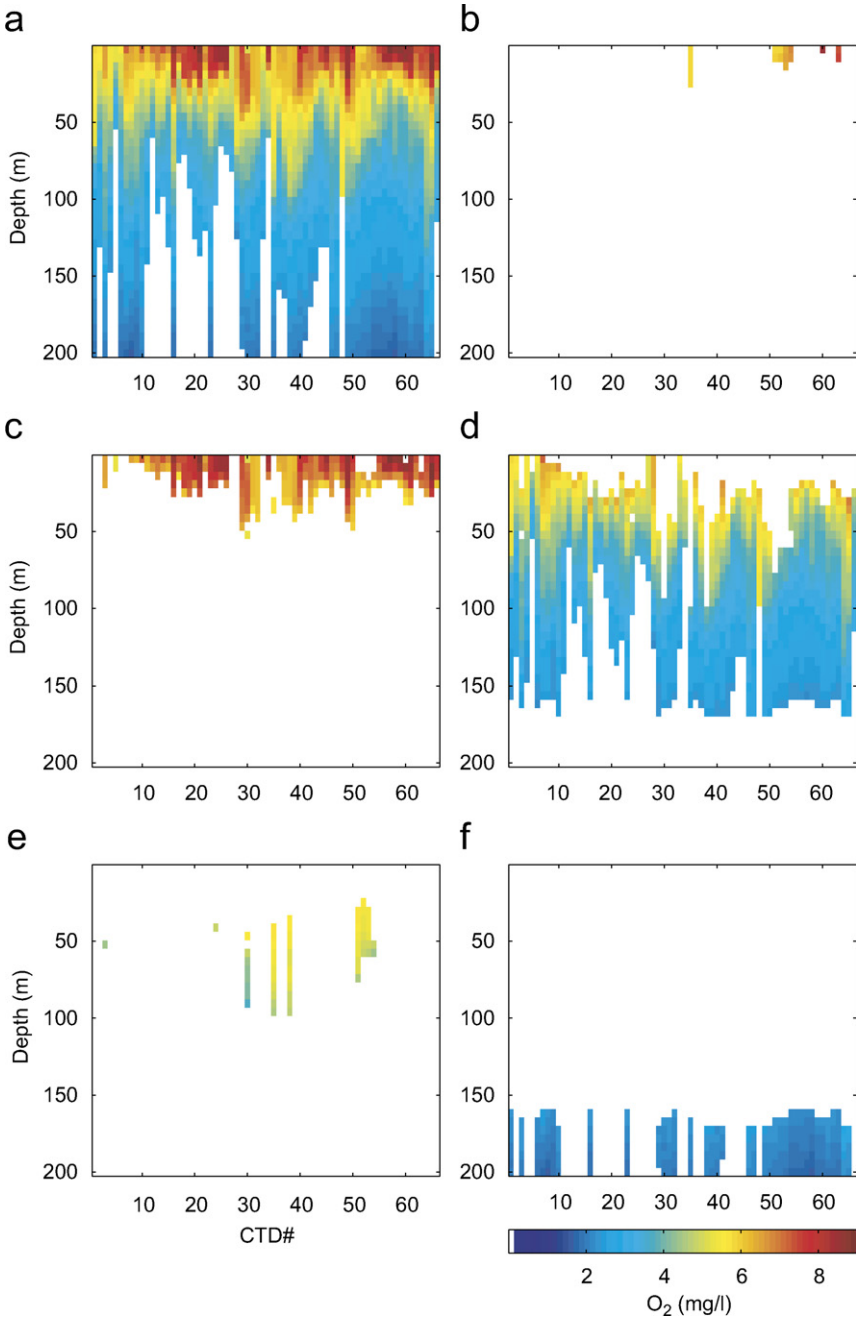

Fig. 5. O_2 distributions at CTD stations: (a) O_2 distribution in water column, (b) O_2 for BWW, (c) O_2 for BSW, (d) O_2 for BIW, (e) O_2 for SUW, and (f) O_2 for NPDW.

temperatures (Fig. 3) suggest a solar event in the fringe area.

2.5. Oxygen concentration

The measured oxygen content at the CTD stations is displayed in Fig. 5(a). In the top 20 m, it is within a range of about 5–9 mg/l. Pockets of high oxygen concentration are found in the upper Monterey Bay and along the coast from Pt. Ano Neuvo to Santa Cruz (Stations 15–25); in near-shelf region along 36.95 N (stations 38–45), and further offshore along the western transect (stations 51–61). The internal tide could be the

cause of the near surface oxygen layer variations, from about 25 to 70 m, at CTD stations 51–61. Below depths of about 150 m, the concentration shows little variability.

Another way to look at oxygen distribution and variability is to consider the oxygen content of the individual water masses (Fig. 5b–f). The surface water, BSW in Fig. 5(c), exhibits a variability among the CTD station from 5.07 to 8.98 with a mean of 7.02, as recorded in Table 2. The warm surface water, BWW, mass has a mean oxygen content of 6.41 with a range of 5.8–8.52 (Fig. 5b). The BIW mass has a mean of 3.73 with the maximum range from 2.21 to 7.20. This shows a decrease in oxygen content from the surface water masses. The sub arctic water has a mean of 5.08 with a range of 3.75–5.75. The sub arctic water overlaps in depth with the BIW water. The SUW mean of 5.08 is larger than the BIW mean of 3.73. The larger mean of the SUW water reflects its fresh water origin. The mean of the NPDW water oxygen content is 2.13 with a range of 1.66–2.86. This is a decrease in oxygen content from the water masses located higher up in the water column. Table 3 lists the mean and rms variability of the oxygen concentrations of these water masses.

3. Water masses and dynamical circulation

3.1. Features of the bay circulation

The Monterey Bay regional circulation can be described in two distinct hydrographic states: Upwelling state (1–3 weeks) and relaxed state (3–6 d). These two periods are related to the prevailing wind patterns and scales forcing such states. During the upwelling periods in summertime, the typical circulation of the region in and around Monterey Bay consists of an upwelling front originating from Pt. Ano Nuevo, a cyclonic circulation in shore of the front in the bay, an anticyclonic eddy-like circulation on the offshore of the upwelling front and another upwelling region off of Pt. Sur. When the wind relaxes, the upwelling reduces, and the offshore eddy-like circulation (presumably part of the California Current meandering flow system) flows into the bay and interacts with the flow over the shelf. These features and some relevant references are listed in Table 1.

For water mass analyses, the CTD stations are grouped into two upwelling (U1, U2) and two relaxed (R1, R2) periods as indicated in Table 2 and discussed in Section 2.1. In what follows, we present an analysis of the water masses during the relaxed and upwelling periods and investigate their existence and pathways using a numerical model simulation during the experimental period.

3.2. Water masses during relaxed periods

CTDs located in the upwelling area of Pt. Ano Nuevo were chosen for analysis in order to represent the area during relaxed periods. The CTDs of the first relaxed period, R1, and some of the second relaxed period were merged together (Section 2.1) for analysis of a relaxed period in a region off Pt. Ano Neuvo. In particular, CTDs 17–19 from R1 and CTDs 34–45 from R2 were grouped together. The cluster analysis (Section 2.2) yielded the previously deduced water masses of BWW, BSW, BIW, SUW, and NPDW. The results are shown in Fig. 6(a) with color-coded water mass data points and water mass ellipses superposed. The water mass data points are those of a subset in Fig. 3. The BIW water mass is represented by a narrower trunk in Fig. 6(a), with fewer branches than in Fig. 3, with green asterics. The SUW water mass has fewer sampling points than in Fig. 3. The surface water masses, BSW and BWW, have less representative points or statistics than in the whole bay region displayed in Fig. 3.

3.3. Water masses during active upwelling periods

We considered in Section 2.1 the CTDs of upwelling period U2. These are the CTDs numbered 27–32 (Table 2). They are located in the expected upwelling plume region off of Pt. Ano Neuvo. U1 casts were not used because they are scattered throughout the bay, away from Pt. Ano Nuevo . The cluster analysis described in Section 2.2, yielded one of the surface water masses, BSW and the BIW, SUW, and NPDW water masses. The BWW water mass was not in the dataset. The results are shown in the T, S diagram of Fig. 6(b). The data points are color-coded as before with the corresponding water mass ellipses superposed. Relative to the relaxed period results shown in Fig. 6(a), there are three branches of BIW in the region. The branching of the BIW water masses from relaxed to the upwelling period is

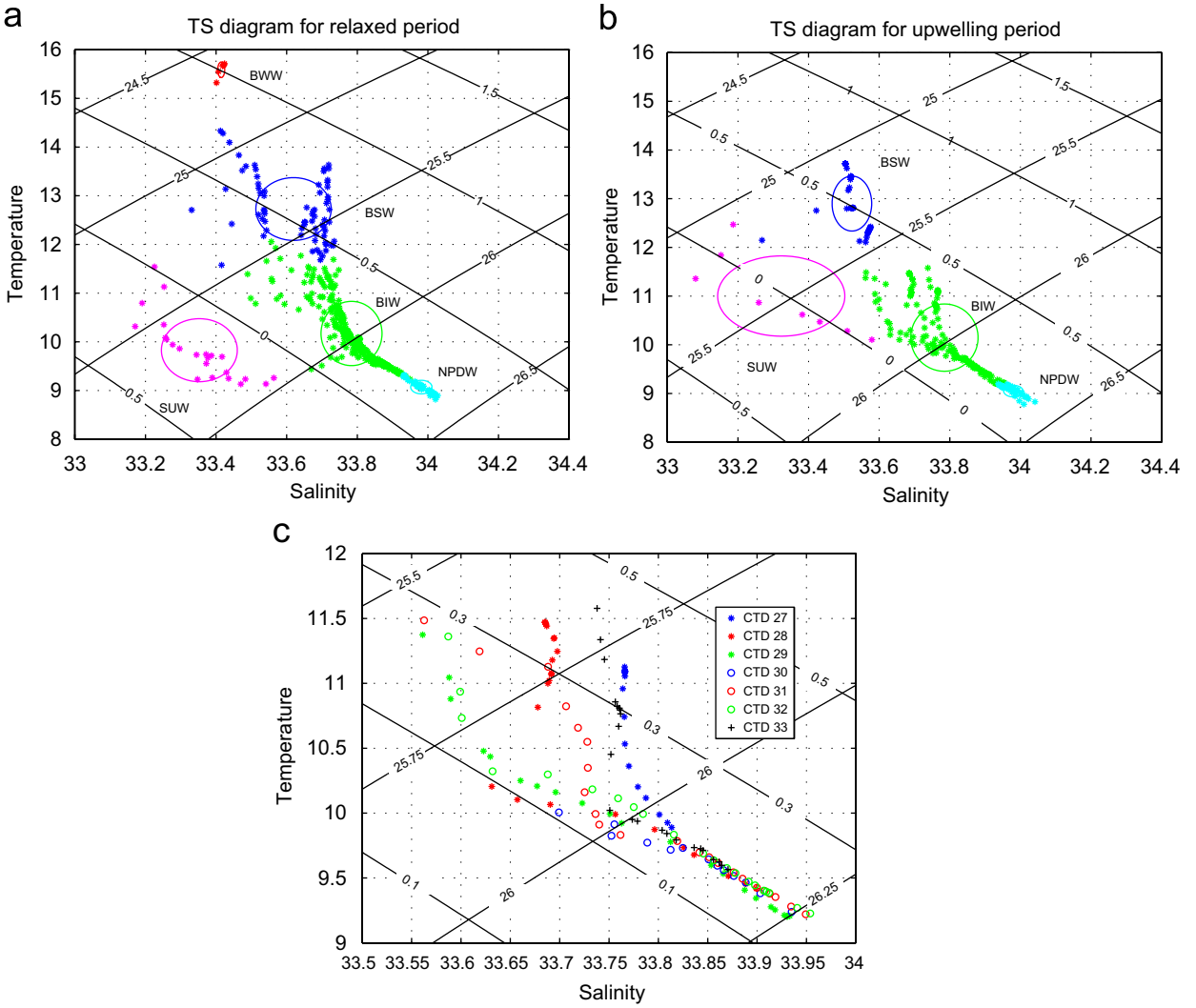

Fig. 6. *TS* diagrams: (a) water masses during relaxed period, (b) water masses during upwelling period, and (c) *TS* distributions at CDT stations 27–33 for BIW mass.

investigated later with help of innovative coastal observation network (ICON) model simulations in Section 4.1. In Fig. 6(a), the separation in the BSW water masses arises due to different periods before and after upwelling events.

The NPDW mass has the same overall structure as in the relaxed period (Fig. 6a). It, however, has a bifurcation at the bottom into two branches, one slightly more saline than the other. The less saline branch appears in the area during upwelling. There is mixing of the upwelled water masses with the BSW water mass and the advected adjacent water. The eddy, that develops during upwelling, moves warmer more saline near shore water offshore to the upwelled area. On the western side of the eddy, the water is less saline, Fig. 7(a).

The ellipse of the SUW water exhibits during upwelling (Fig. 6b), a warming and slight decrease in salinity (11.00, 33.32) relative to the relaxed period (9.83, 33.35) (see Fig. 6a). This water, SUW, lies in the outer fringes of the Monterey Bay area, and is associated with the advection of sub arctic water in the region.

4. Dynamical interpretation of the water mass distribution

As we have seen so far, the water mass analyses during the relaxed and upwelling periods indicate

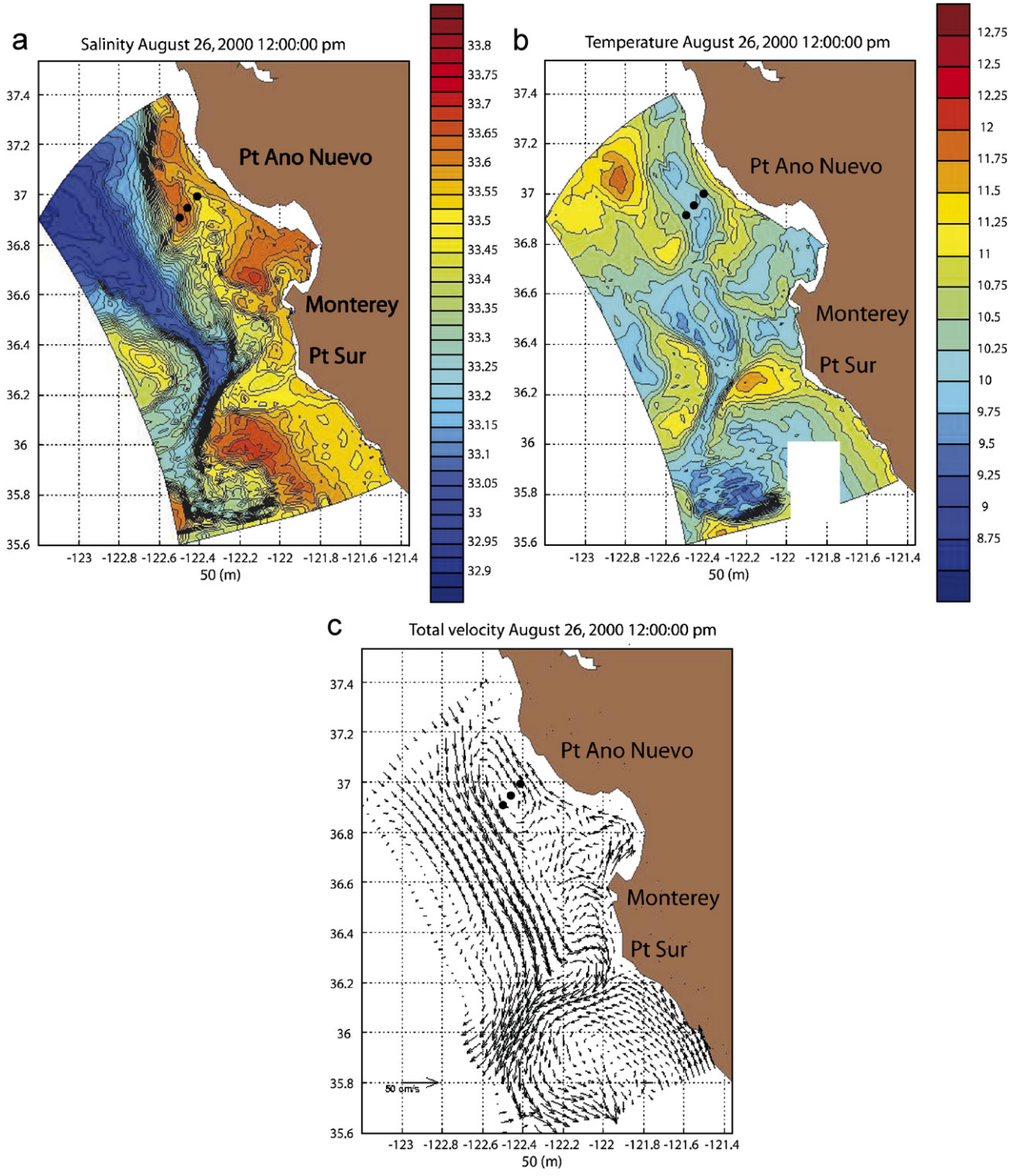

Fig. 7. ICON model predictions for the 26 of August 2000 at 50 m. (a) Salinity, (b) temperature and (c) velocity. CTD stations 29, 31 and 32 (off Pt. Ano Nuevo in increasing order) are shown by black dots in (a)–(c).

two interesting events during this period. First, the manifestation of BIW masses in different branches in the *t*–*s* space and its possible linkage to the bay-wide circulation during upwelling and relaxed periods is investigated. Second, the advection of SUW in this region and its modification is described via spiciness.

4.1. The evolution of BIW through different regimes of upwelling and relaxation

The salinity, temperature and circulation predicted with the ICON model (Shulman et al., 2002) for 26 August 2000 are shown in Fig. 7 at a depth of 50 m. The model has a orthogonal curvilinear grid with a resultant variable resolution in the horizontal, ranging from 1 to 4 km. 30 sigma levels are used in the vertical. On the plots, in Fig. 7, are superimposed the locations of CTD stations 29, 31, and 32 (see Fig. 1 and Section 2.1). An analysis of ICON predictions in the upper 100 m indicates that the circulation patterns are similar. In the upwelling front area off Pt. Ano Nuevo, there is a cyclonic circulation. In the bay area, there is cyclonic circulation in the surface layer, Fig. 7(c). Below the surface at intermediate depths the flow is anticyclonic (Garcia, 1971). An anticyclonic flow at intermediate depths is consistent with inflow from the north into the bay (Brunner, 1988). Further offshore, the circulation is anti-cyclonic and part of the meandering CC (Fig. 7c). In the southern region, on the other hand, there is a large cyclonic component.

The horizontal temperature and salinity distributions (Figs. 7a and b), show a cold and saline upwelled area off Pt. Ano Nuevo. The salinity contours of Fig. 7b indicate the boundaries of the upwelled plume type front. To the right of CTD station 31, a front is located. Past the front there is a lower salinity area and cyclonic circulation in the form of a bulge that pushes lower salinity water towards the shore (Figs. 1 and 7c).

The *TS* diagram structure for the upwelling period (Fig. 6b) provides the temperature and salinity distribution during an upwelling event U2 (Table 2). The BIW water tends to have three branches from its trunk (Fig. 6b), left, middle and right. The CTD stations distribution ranges from 27 to 32 (Table 2). An association of BIW water with CTD station location is provided in Fig. 6c and indicates the presence of BIW water at all stations during upwelling.

The right branch in Fig. 6c consists of CTD stations 27 and 33. These stations are near the coast (Fig. 1). There, the more saline water comes up to the surface during upwelling events.

To understand the origin of the two branches further to the left in the *TS* diagrams of Figs. 6(b) and (c), consider the predicted circulation by the ICON model in the surface region. Fig. 8 displays the predicted circulation on 22, 25, 26, and 28 August 2000.

A cartoon that highlights the events of concern for the circulation is superposed. Fig. 8(a) shows a cyclonic trend off Pt. Ano Nuevo during the beginning of the relaxed period, Table 2. Then the wind starts the upwelling process by generating an offshore Ekman velocity that results in an eddy off of Pt. Ano Nuevo (Fig. 8b). At this time, the cold upwelled water appears off Pt. Ano Nuevo as well. In a day, the eddy moves southwest, towards the prevailing southerly current and weakens (Fig. 8c). As the wind diminishes, the eddy becomes more elongated in the north–south direction and is absorbed by the southerly current (Fig. 8d). The generation of the eddy is a signature of the upwelling event and it's disappearance marks the end of this event.

The second branch from the right in Fig. 6(c) contains contributions from CTDs 28 (red asterisk) and 31 (red circle). The top part of the CTD 28 curve, extending from about 10.75 to 11.5 C, represents upwelled water that has been advected and modified through mixing. Below the top part is the original water with a T, S relation that existed before the upwelling event. It is worth investigating when the mixing stops in the vertical from this cast. Note that the bottom water T–S lies on a constant spice line (0.2). The upper level waters span a range of spiciness values, indicting vigorous mixing due to surface forcing. As postulated by Stern (1967), the action of salt fingers on spice anomalies is to cause warm salty anomalies to rise across density surfaces, because they lose more salt than heat. The cold fresh anomalies will sink across the density surfaces because they gain more salt than heat. The mixing continues until anomalies disappear. In the current situation with CTD 28, the upper layer will continue mixing in the salt fingering mode till the bottom of the upper layer reaches the same density as that of the layer below. Thus, the mixing will stop when the upper water and the lower layer finds a constant isopycnal surface. In this case it is the $\sigma_T = 25.7$ line. From Fig. 9(a), which shows the density profile of the nearest CTD (♯29) , this isopycnal surface is at a depth around 40 m. Note the sharp change of spiciness above and below this depth. This is the depth where mixing will stop between the two water masses of different spiciness but having same density.

Consider the water mass variability in an eddy and correspondingly in T, S characteristics. CTD

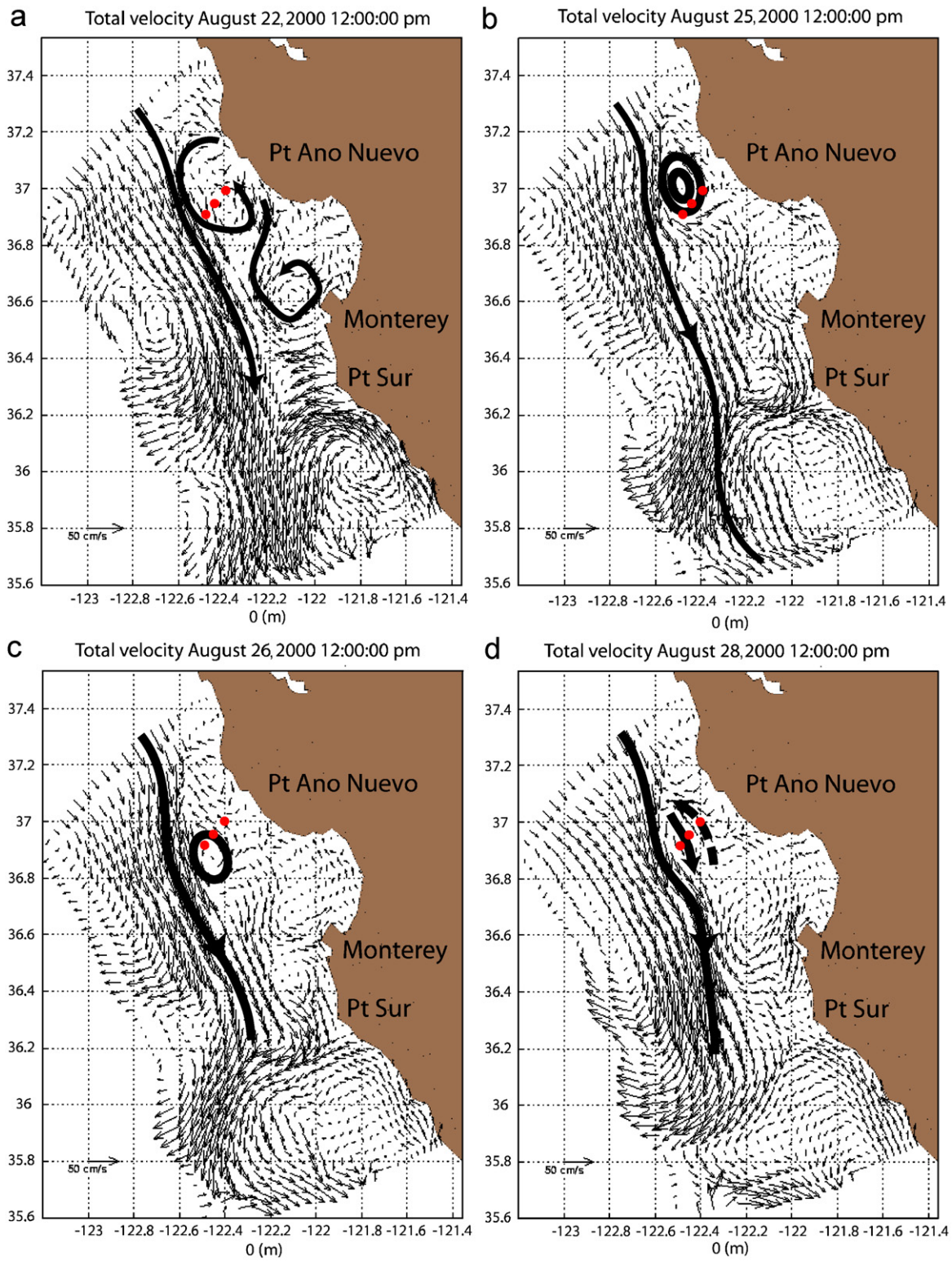

Fig. 8. Surface circulation predictions with the ICON model for: (a) 22 August 2000, (b) 25 August 2000, (c) 26 August 2000 and (d) 28 August 2000. Sketched lines emphasize features. Solid red circles show CTD stations as in Fig. 7.

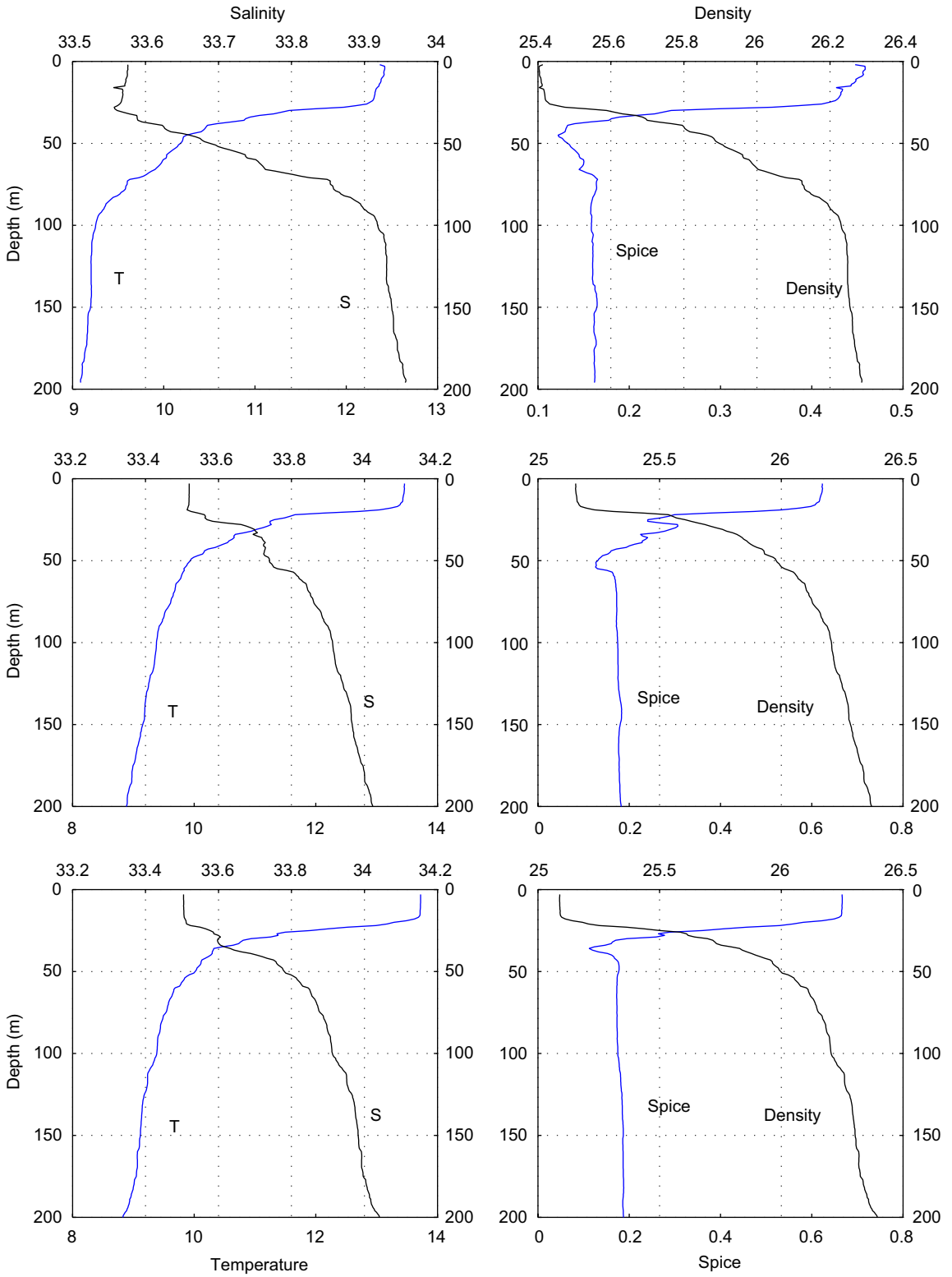

Fig. 9. Temperature, salinity, density and spiciness profiles at CTD stations 29, 31 and 32. Top of page from left to right CTD stations 29, middle of page CTD station 31 and bottom of page CTD station 32.

station 31 is located in the center region of an eddy that is generated during the upwelling period (Fig. 8b). BIW water mass variations inside the eddy are shown in Fig. 6(c) by the red circles. The T, S distribution exhibits from top to bottom four regions, located from 11.5 to 11.2 C, 11.2 to 10.5 C, 10.5 to 10.0 C and 10.0 to 9.2 C. The four regions extent from the left to the right boundaries of the T, S diagram domain, indicating a large variability. This reflects the wide range of water mass characteristics variability caused an eddy and its circulation.

CTD 32 is located to the left side of the eddy (Figs. 1, 7b and 8b). The green circles in Fig. 6(c) show its T, S distribution. This distribution is part of the third branch from the right in Fig. 6(c). The local circulation is in the direction of the southwards flow along the coast. In this area the water is less saline (Fig. 7a). The water there is warmer than in the upwelled core (Fig. 7b).

CTD 29 is located on the right side of the eddy (Figs. 1 and 8b). Its T, S distribution is part of the third branch from the right (Fig. 6c). This is a situation where the cyclonic circulation is around the eddy (Fig. 8b), and thus brings the water masses from the left side of the eddy to the right. As a result, we see the same characteristic T, S distribution on both sides. This is also evident in Figs. 7(a) and (b).

CTD 30 is located towards the right side of the eddy (Figs. 1, 7c and 8b). There, the cyclonic circulation tends to move the water from left to right. The resultant BIW branch (blue circle in Fig. 6c) lays on the left limit of the BIW water distribution in Fig. 6(b), together with CTD's 29 and 32.

4.2. The advection of SUW in the Monterey Bay region

The SUW water is advected into the region by the California along-shore current that flows southwards, Fig. 8. Eddies that are formed on the inshore side of the coastal current could advect the SUW closer to the shore.

The SUW water is not very abundant. It occupies only 1.4% of the volume at analyzed CTD stations and appears at few of them (Fig. 4a). One place where it does appear during upwelling is CTD station 30 (Table 2 and Fig. 4). The pink SUW branch in Fig. 6(b) is from CTD station 30.

An understanding of the modification that the SUW water undergoes in the region can be obtained by considering a model salinity prediction at 50 m for 26 August 2000 (Fig. 7). CTD station 30 (Fig. 1) is on the fringe of the plume towards the less saline area to the right of it (Fig. 7a). The SUW water mass undergoes entrainment and mixing in the fringe area of the plume. As a result it becomes warmer and slightly less saline during the upwelling period (Fig. 6b) than in the relaxed period (Fig. 6a).

The SUW water tends to be located in a shallow layer below the surface (Table 2). There it undergoes mixing with the BWW and BIW water masses. The SUW water tends to form a branch of it own with a distinct spiciness value of around -0.15 (Table 2 and Fig. 3). During periods of upwelling the spiciness value increases and hover around 0 (Fig. 6a). During relaxed periods the spiciness is negative and fluctuates around -0.15. The increase in spiciness during upwelling is caused by mixing that results in warming and slight change in salinity.

4.3. Water mass distribution in eddy area

During the upwelling period U2 (Table 2) an eddy develops off Pt. Ano Nuevo. The ICON model prediction for 26 August 2000 illustrates this eddy and the associated regional circulation, temperature and salinity (Fig. 7). Superimposed on the plots are CTD stations 29, 31, and 32 that were taken during the upwelling period U2 (Table 2).

Fig. 9 shows the temperature, salinity, density and spiciness at the CTD stations. The temperature profiles contain a mixed layer, thermocline and a decreasing temperature versus depth. The salinity profiles show a mixed layer, a halocline and an increasing salinity versus depth. The density profiles reflect the temperature and salinity distributions. The density distribution is stable in depth.

Below about 70 m, the spiciness profiles tend to be constant. At shallower depths, or below a salinity of around 33.8 psi, the BIW spiciness varies (Fig. 6b). The variation, in terms of a decrease and an increase, is evident in Fig. 9 as one proceeds from depth to the surface. As the surface is approached the spiciness values increases and then tends to become constant in the mixed layer. This is the region of the BSW (Fig. 6b).

CTD 31 is in the center region of the eddy and exhibits a mixed region for salinity in the halocline.

The salinity in the mixed region is around 33.7 ppt. The existence of such a region below the surface, suggests mixing of BSW and BIW water masses (Table 4). The spiciness oscillations around 25 m are also suggestive of mixing between the BSW and BIW water masses.

4.4. Spiciness signature of water mass

The spiciness distribution at the CTD stations is shown in Fig. 10 as a function of depth and as a function of water mass versus depth. The CTD stations are numbered as in Fig. 1, where the geographical location is indicated. Fig. 10(a) exhibits the spiciness at each of the CTD stations. The white background corresponds to no data locations. The values vary from around 1 to −0.2 in agreement with Fig. 3. The high values of spiciness are in the surface region. From the surface downwards, the spiciness decreases. At deeper depths the spiciness value is more homogeneous and has less variation versus depth. BWW (Fig. 10b) has the highest spiciness values that are concentrated at a few locations, mostly at the outskirts of the region. BSW has also high spiciness values with comparable magnitudes to BWW (Fig. 10c). BSW is found throughout the domain (Fig. 4) and its high spiciness reaches down to 50 m. The most dominant water, BIW has spiciness values around 0.2 (Table 3 and Fig. 10d). BIW is generally below the surface with some exceptions (Fig. 4a). The spiciness distribution of BIW has the largest extent in the water column among all the waters. The spiciness values of the BIW water tend to connect with the NPDW water at depth (Figs. 10f and 3). The trunks of the BIW and NPDW merge (Fig. 3) with spiciness approaching about 0.18 (Table 3). The NPDW occupies the bottom of the water column and exhibits little variation in spiciness. The SUW (Fig. 10e) has the lowest spiciness value, among all the water masses, of about −0.15 (Table 3). This value of −0.15 is a distinct indicator of sub arctic water in the region that is located between about 30 and 100 m.

5. Conclusion

We conducted a cluster water mass analysis of the MUSE 2000 CTD dataset. We showed that the dataset contains five water masses. These are BSW, BWW, BIW, SUW and NPDW. The BWW is a new water mass that exists during the time span of the data, with unique T, S and spiciness values, and is attributed to the effects of solar heating.

The BIW water is the most dominant water mass and occupies 68.8% of the volume. The next most dominant water mass is NPWD, with 19.5% of the volume. After that follows BSW with 9.9% of the volume, SUW with 1.4% of the volume, and BWW with 0.4% of the volume.

The statistical means and standard deviations for each water parameter and oxygen were calculated. The SUW water mass had a higher oxygen content than the surrounding water masses at similar depths. This reflected the freshwater origin of the SUW water mass. Pockets of high oxygen concentration near the coast, off the coast and on the fringes of the bay exist.

The water mass content and structure was analyzed and studied during upwelling and a relaxed period. While all of the water types were present in the relaxed period, BWW was absent during the upwelling phase. There was also a distinct warming and freshening of the SUW during the relaxed phase compared to its signature during upwelling. In other words, the SUW was ''spiced'' up during relaxation. Off Pt. Ano Nuevo the ICON model showed the formation of a cyclonic eddy during the analyzed upwelling period. The formation of the eddy was in the area where the CTD data indicated the occurrence of the upwelling core. In time, the eddy moved southwest and became absorbed into the southerly flow. The absorption overlapped with the beginning of the relaxed period.

During upwelling, along a CTD track off Pt. Ano Nuevo, the water mass T, S distribution tended to be organized along three branches. The right branch corresponded to the upwelled water near the coast. The central branch reflected some of the variability that exists in the core of the eddy. The CTD station in the center of the eddy core indicated maximum T, S variability that reached adjacent branches in some regions. The CTD stations at the fringes of the eddy exhibited a lower salinity that occurred in the southerly flow away from the coast and their T, S values lay on the left branch.

The highest values of spiciness occur in the surface region, with constant values in the mixed layer. From the surface downwards the spiciness values decrease. The SUW has a distinct negative spiciness (about −0.20), which should uniquely define this water mass in all future experiments. The spiciness distribution of BIW water has the

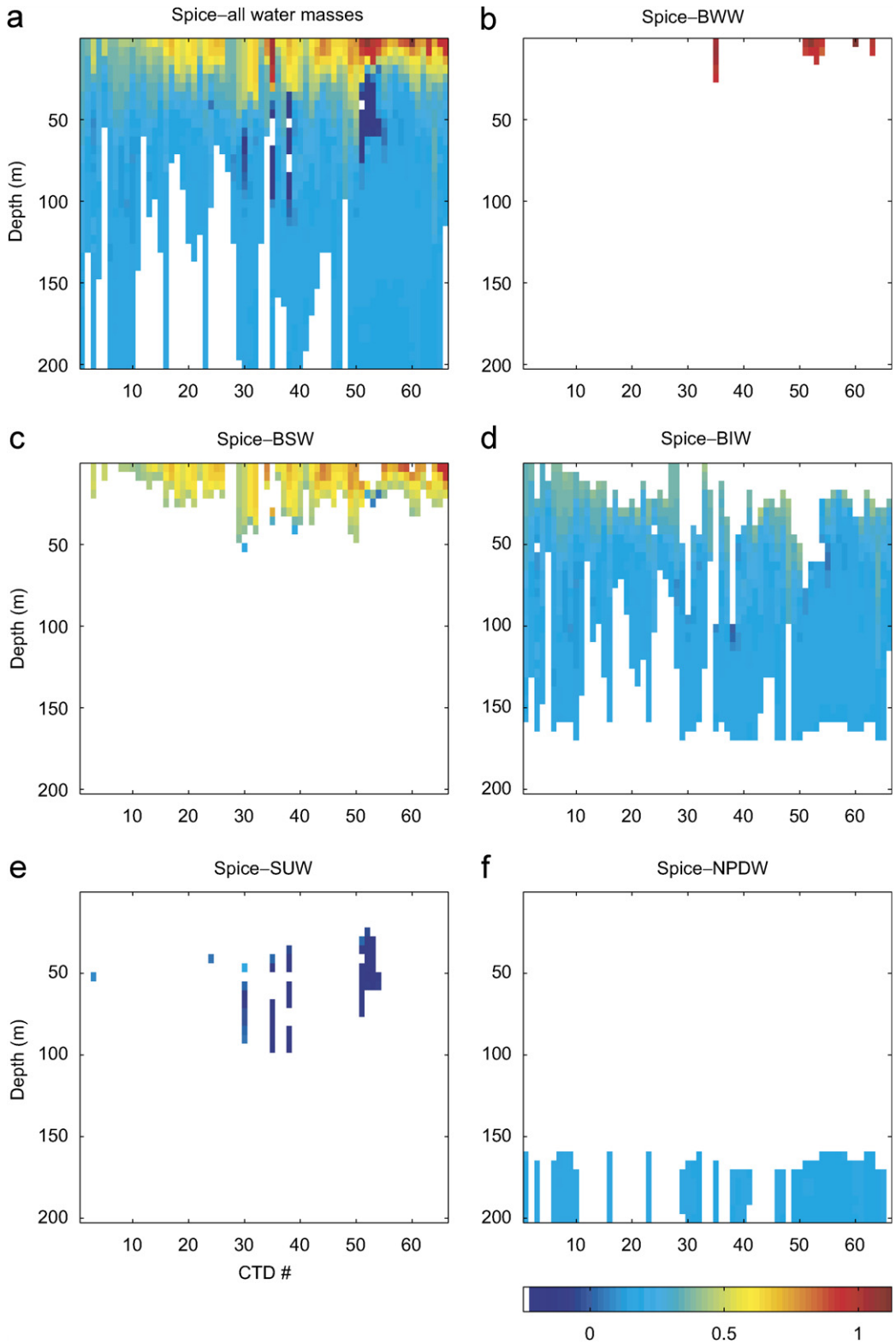

Fig. 10. Spiciness versus depth at the CTD stations. Top of page from left to right (a and b) all water masses and BWW water mass, middle of page BSW and BIW water masses (c and d) and bottom of page SUW and NPDW water masses (e and f).

largest extent in the water column. The top extent of the BIW water and the surface water masses, BSW and BWW, exhibit the largest spiciness variability. At depth the spiciness values of BIW water tend to be constant and merge with the values of the NPDW water.

Acknowledgments

We gratefully acknowledge the many helpful suggestions made by various colleagues.

This work was supported by the Office of Naval Research under PE 62435N, with technical management provided by the Naval Research Laboratory. AG was partially funded by the Office of Naval Research Grants N00014-03-1-0411 and N00014-03-1-0206 at the University of Massachusetts Dartmouth. Our thanks to Dr. Igor Shulman for making the ICON model predictions available through the Internet (www.deas.harvard.edu/~leslie). Our thanks to the MBARI staff and scientists for making the MUSE 2000 data available to us.

References

Breaker, L.C., Broenkow, W.W., 1994. The circulation of Monterey Bay and related processes. In: Ansell, A.D., Gibson, R.N., Barnes, M. (Eds.), Oceanography and Marine Biology: An Annual Review, vol. 32. UCL Press, London, pp. 1–64.

Brink, K.H., Beardsley, R.C., Niller, P.P., Abbott, M., Huyer, A., Ramp, S., Stanton, T., Stuart, D., 1991. Statistical properties of near-surface flow in the California coastal transition zone. Journal of Geophysical Research 96, 14693–14706.

Brunner, G.M., 1988. Experimental verification of AUV (autonomous underwater vehicle) performance. Naval Postgraduate School Master's Thesis, Monterey.

Ferrari, R., Rudnick, D.L., 2000. Thermohaline variability in the upper ocean. Journal of Geophysical Research 105, 16857–16883.

Flament, P., 2002. A state variable for characterizing water masses and their diffusive stability: spiciness. Progress in Oceanography 54, 493–501.

Flament, P., 1986. Finestructure and subduction associated with upwelling filaments. Ph.D. Dissertation, University of California San Diego.

Fofonoff, N.P., 1985. Physical properties of seawater: a new salinity scale and equation of state for sea-water. Journal of Geophysical Research 90, 3332–3343.

Gangopadhyay, A., Kim, H.S., Mukherjee, G., Leslie, W.G., Haley Jr., P.J., Lermusiaux, P.F.J., Robinson, A.R., Rosenfeld, L.K., 2006. Development of a feature-oriented regional modeling system (FORMS) for the California Current System, in preparation.

Garcia, R.A., 1971. Numerical simulation of currents in Monterey Bay. MS Thesis, Naval Postgraduate School, Monterey.

Hickey, B.M., 1979. The California current system—hypothesis and facts. Progress in Oceanography 8, 191–279.

Hickey, B.M., 1997. The response of a steep-sided, narrow canyon to time-variable wind forcing. Journal of Physical Oceanography 25 (5), 697–726.

Kim, K., Kim, K.R., Rhee, T.S., Rho, H.K., 1991. Identification of water masses in the YS and East China Sea by cluster analysis. In: Takano, K. (Ed.), Oceanography of Asian Marginal Seas. Elsevier, Amsterdam, pp. 253–267.

Lien, R.C., Gregg, M.C., 2001. Observations of turbulence in a tidal beam and across a coastal ridge. Journal of Geophysical Research 106 (C3), 4575–4591.

Mied, R.P., McWilliams, J.C., Lindemann, G.J., 1991. The generation and evolution of mushroom-like vortices. Journal of Physical Oceanography 21, 490–510.

Niiler, P.P., Poulain, P.-M., Haury, L.R., 1989. Synoptic three-dimensional circulation in an onshore-flowing filament of the California current. Deep Sea Research 36 (3), 385–405.

Petruncio, E.T., Rosenfeld, L.K., Paduan, J.D., 1998. Observations of the internal tide in Monterey Canyon. Journal of Physical Oceanography 28, 1873–1903.

Ramp, S.R., Rosenfeld, L.K., Tisch, T.D., Hicks, M.R., 1997. Moored observations of the current and temperature structure over the continental slope off central California. Part I: a basic description of the variability. Journal of Geophysical Research 102, 22877–22902.

Rosenfeld, L.K., Schwing, F.B., Garfield, N., Tracy, D.E., 1994. Bifurcated flow from an upwelling center: a cold water source for Monterey Bay. Continental Shelf Research 14, 931–964.

Rosenfeld, L.K., Anderson, T., Hatcher, G., Roughgarden, J., Shkedy, Y., 1995. Upwelling fronts and barnacle recruitment in Central California, MBARI Technical Report 95-19.

Rudnick, D.L., Ferrari, R., 1999. Compensation of horizontal temperature and salinity gradients in the ocean mixed layer. Science 283, 526–529.

Shea, R.E., Broenkow, W.W., 1982. The role of internal tides in the nutrient enrichment of Monterey Bay, California. Esturine, Coastal and Shelf Science 15, 57–66.

Shulman, I., Wu, C.R., Lewis, J.K., Paduan, J.D., Rosenfeld, L.K., Kindle, J.C., Ramp, S.R., Collins, C.A.A., 2002. High resolution modeling and data assimilation in the Monterey Bay area. Continental Shelf Research 22, 1129–1151.

Stern, M.E., 1967. Lateral mixing of water masses. Deep Sea Research Oceanography Abstract 14, 747–753.

Strub, P.T., Kosro, P.M., Huyer, A., 1991. The nature of the cold filaments in the California Current System. Journal of Geophysical Research 96 (C8), 14743–14768.

Tisch, T.D., Ramp, S.R., 1997. Moored observations of the current and temperature structure over the continental slope off central California, 2. The energetics of the flow off Point Sur. Journal of Geophysical Research 102, 22903–22920.

Tomczak, M., Godfrey, J.S., 1994. Regional Oceanography: An Introduction, second ed. Daya Books, New Delhi, India, 390p.

Tracy, D.E., 1990. Source of cold water in Monterey Bay observed by AVHRR satellite imagery. Naval Postgraduate School Master's Thesis, Monterey.

Traganza, E.D., Conrad, J.C., Breaker, L.C., 1981. Satellite observations of a cyclonic upwelling system and giant plume in the California Current. In: Richards, F.A. (Ed.), Coastal Upwelling. American Geophysical Union, Washington, DC, pp. 228–241.

Veronis, G., 1972. On properties of seawater defined by temperature, salinity, and pressure. Journal of Marine Research 30, 227–255.

Warn-Varnas, Gangopadhyay, A., Hawkins, J., Robinson, A., 2005. Wilkinson basin area water masses: a revisit with EOFs. Continental Shelf Research 25, 277–296.